Finite Element Analysis of the Effects of Package Induced Stress on Micromechanical Resonator Temperature Stability

Divya Kashyap

Electrical Engineering and Computer Sciences
University of California at Berkeley

Technical Report No. UCB/EECS-2015-45
http://www.eecs.berkeley.edu/Pubs/TechRpts/2015/EECS-2015-45.html

May 4, 2015

Copyright © 2015, by the author(s).
All rights reserved.

Permission to make digital or hard copies of all or part of this work for personal or classroom use is granted without fee provided that copies are not made or distributed for profit or commercial advantage and that copies bear this notice and the full citation on the first page. To copy otherwise, to republish, to post on servers or to redistribute to lists, requires prior specific permission.

Finite Element Analysis of the Effects of Package Induced Stress on Micromechanical Resonator Temperature Stability

by Divya Kashyap

Research Project

Submitted to the Department of Electrical Engineering and Computer Sciences, University of California at Berkeley, in partial satisfaction of the requirements for the degree of **Master of Science, Plan II**.

Approval for the Report and Comprehensive Examination:

Committee:

____

Professor Clark T.-C. Nguyen
Research Advisor

____

(Date)

* * * * * * *

____

Professor Liwei Lin
Second Reader

____

(Date)

Table of Contents

Table of Contents ii
Acknowledgements iii
Abstract iv
Introduction 1
Finite Element Analysis 5
  Static Structural analysis of the package model 5
  Strain on the surface of packaged die at -45 °C 7
    Boundary Conditions and Applied loads 7
    Determining resonator anchor displacement expressions 7
    Plastic Encapsulation 9
    Die Attach 9
    Wafer Level Bond 10
    Low Pressure Chemical Vapor Deposition (LPCVD) of Polysilicon 11
    Total Lateral Deformation at -45 °C 11
  Strain of packaged die across the operational temperature range 12
  Temperature dependence of resonant frequency 14
Temperature Stability Results 20
Conclusion 21
References 25
Appendix A 27
Appendix B 28
Appendix C 29

Acknowledgements

I would like to take this opportunity to express my deepest gratitude to my advisor, Professor Clark Nguyen, for his guidance on this research project. He gave me the freedom to choose any approach toward the goal he had set, while steering me in the direction that would make my work meaningful. He has been very appreciative of my efforts, especially my writing skills. Not only is he very knowledgeable, but also quite patient when explaining even the simplest of topics, the hallmark of a great teacher. His presentations always inspired me and I learned a lot from his lectures, and more from the homework and projects assigned. Speaking of which, I am very fortunate to have had the help of great GSIs, Jalal Naghsh Nilchi and Henry Barrow. Having the same instructors for coursework and research helped me understand the connection between circuit design and MEMS. Special thanks goes to Jalal, who, along with Ruonan Liu, took the time to clarify some of the basic concepts I would frequently miss.

I want to thank Mehmet Akgul and Thura Lin Naing for giving me suggestions and tips on my simulation. To the rest of the Nguyen group, Alper Ozgurluk, Tristan Rocheleau, Robert A. Schneider, Wei-Chang Li, Turker Beyazoglu, Lingqi Wu, and Yang Lin, thanks for being curious about my project. Trying to answer all your questions led me to so much information which will be very useful in my career.

I'm very grateful for all the work BSAC does in order to convey our research to industry and the biannual IAB Research Review. And of course, I'm an ardent fan of the lunch seminars!

I'm honored to have been the recipient of the Chancellor's Fellowship for Graduate Study provided by the Graduate Division at Cal. Their financial support has been of great help.

Last but not the least, I would like to thank my parents for standing by me all these years, my dad for being a smart engineer and helping me with math and science throughout school, and my mom for her unconditional love and words of encouragement. I am truly awed and inspired by the creativity of my sister, Shreya, whose blog posts and drawings are something I always look forward to, in addition to parodies of the latest hit songs. I have no doubt she'll be the coolest doctor on this planet! To all the other friends I've made at Berkeley, thanks for being part of this wonderful journey. If I had to include everyone here, the list would be endless.

Abstract

Vacuum encapsulation of RF disk and beam resonators is often needed to maintain high quality factor and frequency stability. Conventionally, this is performed at the wafer level by anodic, eutectic, fusion, or glass frit bonding. After wafer dicing, packaging proceeds with die attach to the package substrate and plastic over molding. This process leads to many contacts between materials of different coefficients of thermal expansion (CTE) resulting in package-induced stress. The focus of this work is to determine the effect of this stress on the temperature stability of micromechanical resonators via finite element analysis (FEA), for applications that do not require attachment to a printed circuit board, such as the sensors in the original vision of Smart Dust. The simulation is separated into two main parts: (a) package analysis and (b) resonator analysis. The package is analyzed in a static structural environment, recording mesh model nodal displacement on the packaged die surface, yielding displacement boundary conditions specific for each of the selected package models. These boundary conditions are then applied to the anchor nodes of the resonator in a separate prestressed modal analysis to determine modal frequencies of the desired mode shapes. Results indicate that package-induced stress depends mostly on die thickness and die attach CTE. Thinner dies and die attach material with very high CTEs tend to induce more stress in the die. The temperature stability of packaged resonators, when compared to their unpackaged counterparts, is influenced very slightly by the package alone. Thinner dies improve temperature stability very slightly, although there is residual stress in the die itself, which may lead to mechanical failure of the package. Of the resonator geometries investigated, the clamped-clamped beam is the most susceptible to package-induced stress, because of the large anchor contact area to the substrate. The centrally anchored disk, although directly anchored to the substrate, contacts a much smaller area, and thus, its temperature stability is unaffected by package-induced stress. Although it has large anchors, the free-free beam is levitated by support beams, and so, its temperature stability is only slightly affected. Finite element models are solved using the commercial FEA software package ANSYS 14.5.

Introduction

Standard packaging of electronic components after microfabrication on a semiconductor wafer and wafer dicing involves die attach and plastic over molding. MEMS components, however, require additional wafer level encapsulation after microfabrication to allow mechanical movement of the component. In particular, radio frequency MEMS resonators often require vacuum encapsulation for high quality factor and frequency stability. Wafer bonding processes that offer the required hermeticity at the wafer level are anodic, eutectic, fusion, and glass frit bonding [1]. Examples of commercial vacuum packaged MEMS resonators include the Discera oscillator [2] and the InvenSense gyroscope [3].

After singulation, the wafer level encapsulated die is picked up by a vacuum tool, and bonded to the package substrate (can be copper in case a heat sink is required, or more commonly, plastic or ceramic) via an adhesive called the die attach [4]. This step induces the most stress at the surface of the resonator substrate, and has been investigated extensively as to how it affects semiconductor device performance [5]. Using experimental evidence, the authors of [6] have suggested that the stress resulting from die attach can actually be used to compensate the temperature coefficient of frequency of quadruple mass gyroscopes by controlling die bond area. A four-dot die attach approach, as opposed to the full die attach approach, elaborated on in [7], proves to be less detrimental to the performance of an accelerometer. Walwadkar and Cho have looked at the effects of two types of die attach (silver glass and polyimide) on die surface stress [8]. However, a very large die size is used in [5-8], typically required of integrated circuits, accelerometers, and gyroscopes, with each side being several millimeters in length. On the other hand, an RF MEMS resonator (like the one in [9]), its electrodes and contact lines take up much less space, requiring a much smaller die.

Low Temperature Co-fired Ceramic (LTCC) has many electrical and mechanical properties favorable to RF resonators, when compared to other package substrates. It has a low loss tangent at high frequencies. Manufacturing is performed in a multilayer process, so it’s possible to embed passive circuits by printing metal traces such as resistors, capacitors, and inductors, and connecting layers through vias. Due to the low dielectric constant, the parasitic capacitance in these embedded circuits is low, minimizing crosstalk. The thermal expansion coefficient of LTCC is close to that of silicon, lowering package-induced stress on the die surface

[10-12]. When wafer bonding processes are not readily accessible, or for prototype testing, when package size is not of concern, pre-made cavities and lids, manufactured from LTCC, can be used to vacuum seal MEMS resonators, by virtue of its hermetic property [9].

The objective of the simulations in this report is to evaluate the effect of package-induced stress on the temperature coefficient of frequency of the MEMS resonator. The simulations performed are linear static and material properties, listed in Table 1, are linear elastic. The package model chosen for this study measures 2.5 mm × 2.0 mm × 3.5 mm, occupying the same footprint as commercial MEMS oscillators [2]. A dimensioned 2D sketch is provided in Figure 1. Nominal thickness values are used for each component. Since this is meant to be a general package model, electrical leads are ignored. The die size permits the aforementioned wafer bonding techniques (200 μm wide seal ring), is large enough to accommodate the resonator, and can be picked up by standard die collets [13]. Two types of wafer level encapsulation are investigated: (a) silicon-to-silicon glass frit bond and (b) a glass-to-silicon anodic bond. The cavity in the silicon wafer level cap is etched at an angle of 54.7° and bonded to the resonator wafer using glass frit. For anodic bonding, the material properties of the cap wafer are changed to that of Pyrex, and since a thin layer of oxide forms as the interlayer, the material properties of the glass frit layer are replaced with that of oxide. For simplicity, the fact that the pyrex wafer cap may have a rounded profile, unlike anisotropically etched silicon, is ignored. This ensures that the resulting stress values are only a product of material properties, rather than changes in geometry. Three types of die attach are experimented with: (a) silver glass, (b) polyimide, and (c) a standard IC die attach.

Table 1: Properties of materials used in this study of package-induced stress. All materials are linear elastic.

Material	Coefficient of Thermal Expansion [ppm/°C]	Young's Modulus [GPa]	Poisson's Ratio
Silicon	2.85	169 at 22 °C; -60 ppm/°C	0.28
Pyrex	3.25	62.75	0.2
Glass Frit	6.3	50	0.22
Oxide	0.5	70	0.17
Silver glass [8]	16	11.5	0.35
Polyimide [8]	13	2.47	0.4
Standard die attach used in plastic IC packaging [5]	60	5	0.35
Ceramic [12]	5.8	120	0.24
Plastic [5]	15	11.5	0.3
Polysilicon	3.35	150 at 22 °C; -40 ppm/°C	0.226

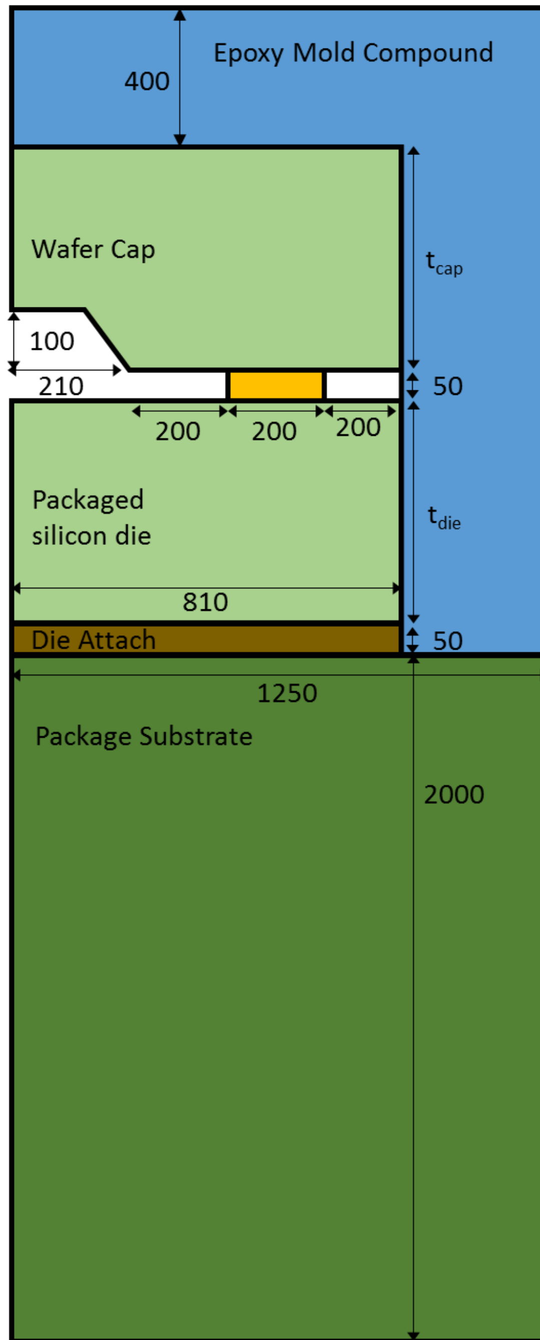

Figure 1: 2D sketch showing dimensions (in µm) of package model.

Preliminary simulations revealed that the following package models are the most interesting both in terms of package-induced stress and the ensuing change in resonator temperature coefficient of frequency.

Table 2: Package models investigated in this study

Package Model	Die Attach Material	Cap Wafer Material	Wafer Bond Material	Packaged die and wafer cap thickness (t_{cap} and t_{die}) [μm]
A	Standard die attach used in plastic IC packaging	Pyrex	Oxide	300
B	Silver glass	Silicon	Glass Frit	300
C	Silver glass	Silicon	Glass Frit	500
D	Polyimide	Silicon	Glass Frit	500
E	Standard die attach used in plastic IC packaging	Silicon	Glass Frit	500
F	Standard die attach used in plastic IC packaging	Pyrex	Oxide	500

The following sections of this report detail the procedure used to simulate resonator temperature stability in packaged and unpackaged resonators, via ANSYS 14.5 [14]. The package models are simulated and the resulting strain boundary conditions are applied to the resonator anchors. Results are presented and the conclusion section interprets the applicability of these results.

Finite Element Analysis

The objective of this study is to determine the effect of package-induced stress on resonator temperature stability by first performing a static structural analysis on the package model and then applying the deformation result to the resonator anchor in a modal analysis, as illustrated in Figure 2. The analysis is split in order to investigate the effect of one package on the behavior of various resonator geometries. In this report, geometries observed are the clamped-clamped beam, free-free beam, center-stem disk, and stemless disk levitated by four support beams.

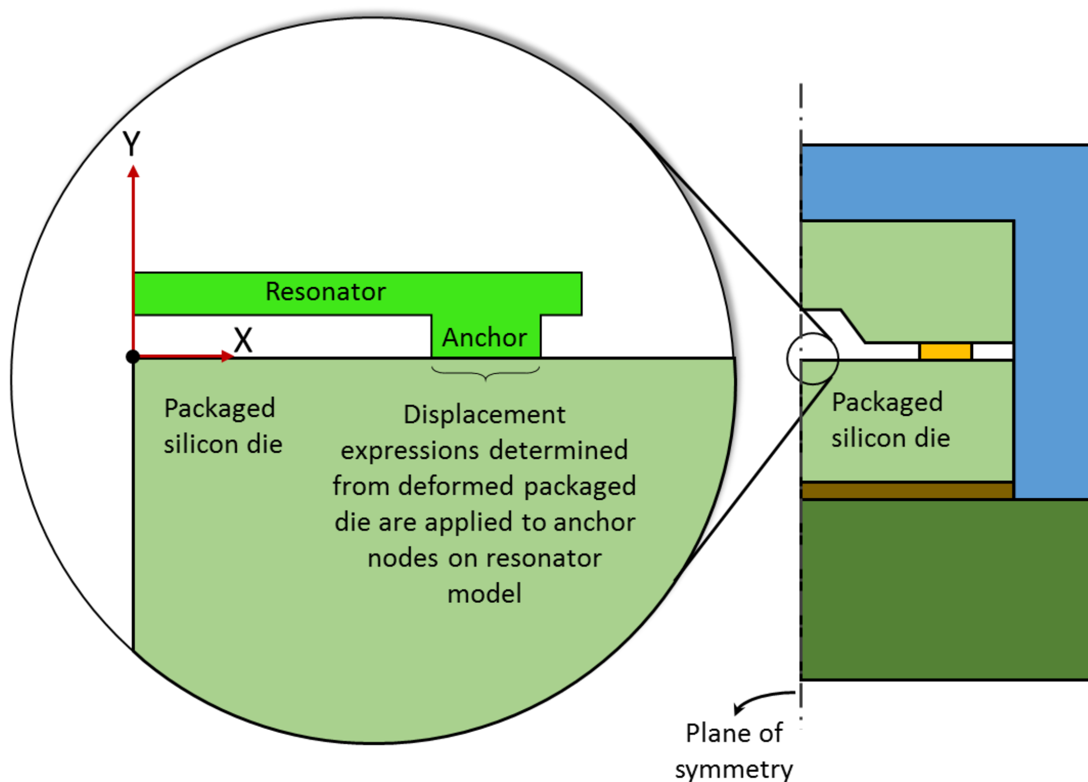

Figure 2: Overview of the analysis carried out in this report. First, the package model (right) is simulated. Then, the displacement observed on the surface of the packaged silicon die is applied as a boundary condition in the modal analysis of the resonator. The zoomed-in view shows where the resonator (clamped-clamped beam in this figure) would be anchored on the die.

Static Structural analysis of the package model

The first step to simulating thermal stability of packaged resonators is developing a model for package induced stress that can be used as a boundary condition for the resonator. Residual stress in the package that deforms the silicon die (resonator substrate) is a result of the contact

between materials of mismatched thermal expansion coefficients and thermal strain from a high stress free temperature. In this report, it is assumed that both the resonators and the silicon die are stress free during deposition, at 600 °C, the nominal temperature for low pressure chemical vapor deposition of polysilicon. The total deformation is a sum of the individual deformations after deposition, wafer level bonding, die attach, and plastic encapsulation. Since the analysis performed for this study is static and neglects large deformation effects, results of multiple steps are independent of each other, i.e., the same sum will be obtained for simulation of the various packaging steps in any order, by the commutative property of addition. Utilizing the birth and death of elements capability (code lines in Appendix B) in ANSYS, static structural analysis on the package model begins with the last step in the package process, plastic encapsulation, and proceeds in reverse, ending with resonator deposition, by selectively killing solid and contact elements not present at the current step. For example, die attach to the ceramic substrate is modeled by killing elements that represent the plastic and its contact to other components of the package. This technique ensures that the same mesh model is used in the entire simulation, by killing elements and changing stress free temperatures through APDL command snippets, allowing the use of the "Solution Combination" feature of ANSYS Mechanical to get total deformation. Also, if the stress free temperature changes, for example, if there is an anneal step in the fabrication process, this involves modifying just one value in the entire simulation.

For all package models simulated, due to the small area of the packaged die (1620 μm x 1620 μm), die warpage is minimal, and hence, only lateral strain is explored. The following section explains the procedure to determine strain at -45 °C on the surface of the resonator substrate. This process is repeated for temperature values until 155 °C in increments of 40 °C.

The main cause of resonator frequency shift is the difference in stiffness due to the temperature dependence of Young's modulus and anchor shift. Essential to all simulations is the accurate calculation of stress, whether in the packaged die or the resonator. Hence, the finite element model uses hexahedral elements, and midside nodes are included to add an extra degree of freedom of deformation on each edge, forcing the quadratic shape function on the element. Such an element is said to be the most accurate in stress calculations, according to literature [15]. The model consists of 20-node hexahedron elements (SOLID186), meshed automatically by

ANSYS Mechanical. The mesh setting is specified as “fine”, or having an element size of 0.25 μm, whichever is smaller. The contact pairs consist of CONTA174 and TARGE170 elements.

Strain on the surface of packaged die at -45 °C

Boundary Conditions and Applied loads

Modeling one quadrant of the package and designating planes of symmetry as frictionless supports, shown in Figure 3, implies symmetry. To prevent rigid body motion and set a reference to measure displacement, the center vertex of the silicon die has been fixed, also shown in Figure 3. The stressed temperature is applied as a thermal load.

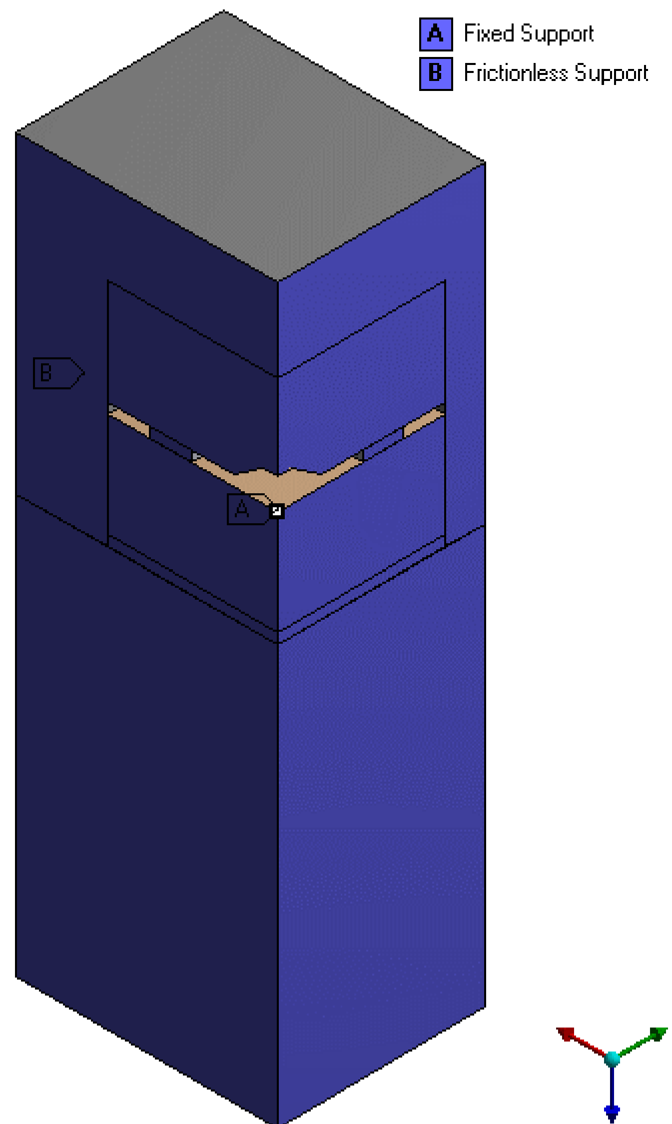

Figure 3: A quadrant of the package model. Planes of symmetry have been designated as frictioness supports and one vertex of the silicon die is fixed to prevent rigid body motion

Determining resonator anchor displacement expressions

Thermal stability simulations assume the resonator is centered on the packaged die. After solving a model with the applied boundary and load conditions, the resulting directional deformation is observed in the region of interest (possible anchor points of the resonator) along the scoped path indicated by the translucent purple arrow in Figure 4. The sum of these displacements from each packaging step is then used to determine strain as a function of temperature. These constraints are then applied as displacement boundary

conditions to the anchors of resonators in a separate model.

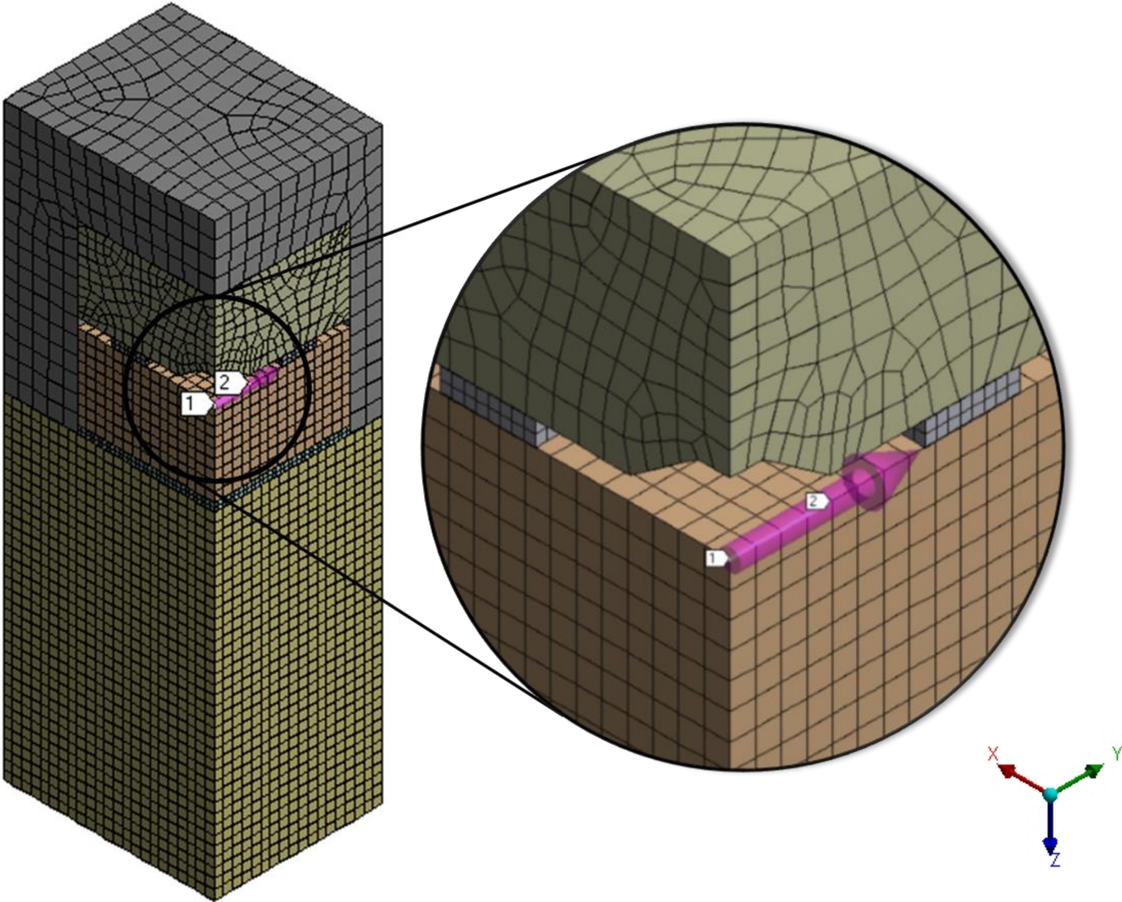

Figure 4: Mesh model of plastic encapsulation step of the packaging process. Deformation in the y-direction along the scoped path (where a resonator would be anchored) is recorded

Plastic Encapsulation

Most thermoplastics cure around 150 °C, so this is chosen as the stress free temperature for plastic encapsulation. To determine packaged strain at -45 °C, the thermal condition applied to all bodies is -45 °C. All solid and contact elements are alive, as shown in Figure 4. The plot on the right shows the y-direction deformation at -45 °C caused by plastic molding along the scoped path.

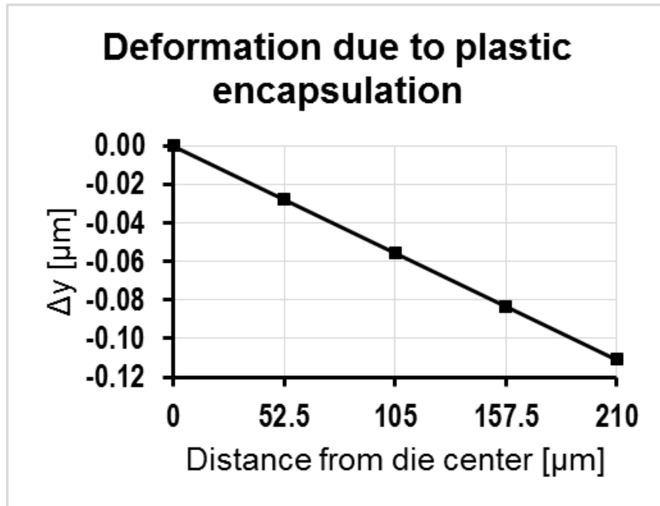

Figure 5: Directional deformation along the y-axis caused by plastic encapsulation

Die Attach

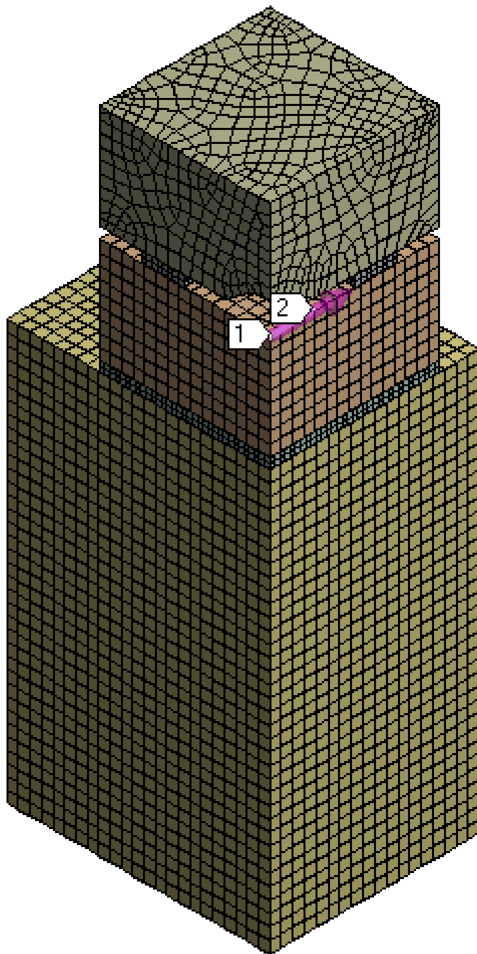

Figure 6: Mesh model of the die attach step

To simulate deformation caused by die attach, the plastic solid elements and its contacts to other bodies are killed. The effective mesh model then looks as shown on the left. The stress free temperature for all elements is chosen to be 350 °C. Since the next step is plastic encapsulation, whose stress free temperature is 150 °C, this is the applied thermal load. Results are plotted below.

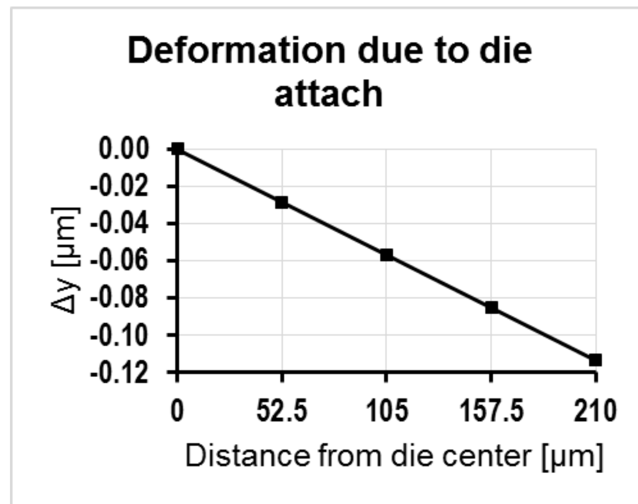

Figure 7: Directional Deformation along y-axis caused by die attach

Wafer Level Bond

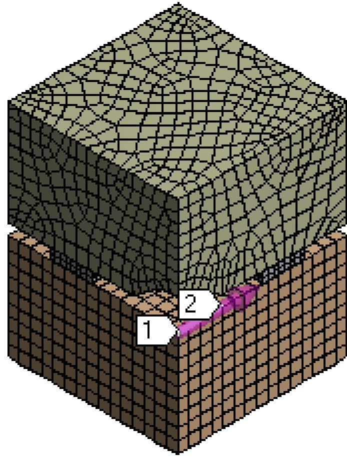

Hermetic wafer level encapsulation, such as anodic and glass frit bonding, normally occurs at 450 °C, the stress free temperature for this step. Since the next step, die attach, happens at 350 °C, this is the applied thermal condition. After killing the plastic, die attach, and ceramic elements and their contacts, the mesh model reduces to the one on the left. Directional deformation results are shown in Figure 9.

Figure 8: Mesh model for wafer level bond

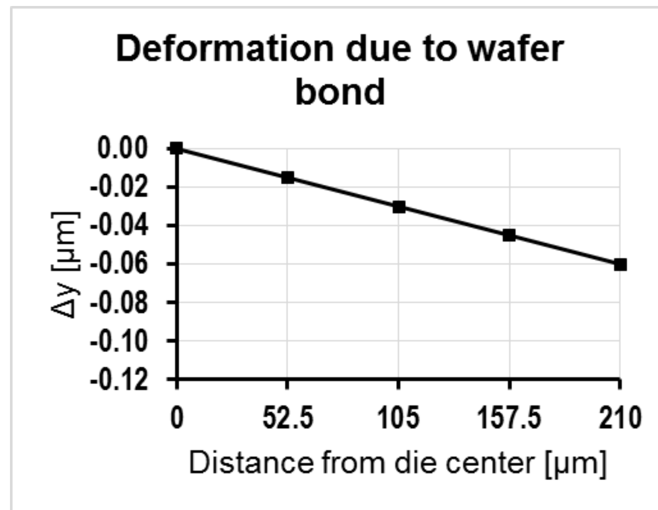

Figure 9: Directional deformation along the y-axis caused by wafer level bond

Low Pressure Chemical Vapor Deposition (LPCVD) of Polysilicon

The structural material for resonators of this work, polysilicon, is deposited at 600 °C, the stress-free temperature for this step. The effective mesh here comprises just the silicon die (Figure 10), and the applied temperature is 450 °C. Directional deformation results are shown in Figure 11.

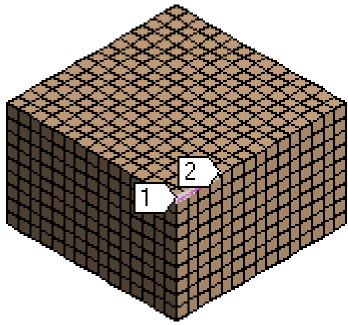

Figure 10: Mesh model for LPCVD

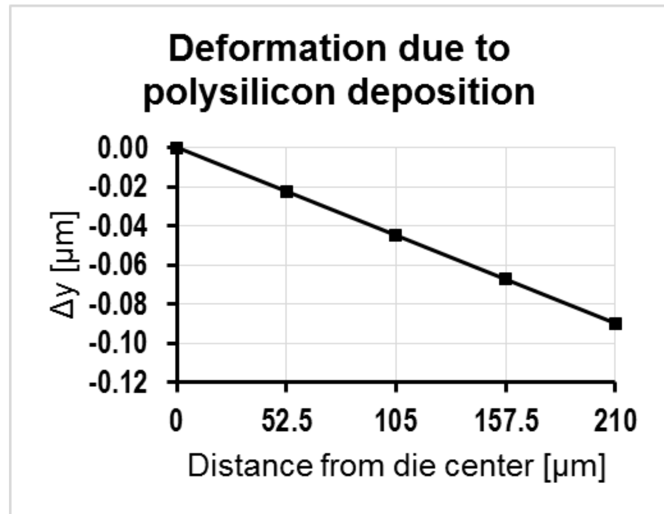

Figure 11: Directional deformation along the y-axis caused by LPCVD

Total Lateral Deformation at -45 °C

Using the "Solution Combination" feature of ANSYS Mechanical, directional deformation from multiple simulations (plastic encapsulation + die attach + wafer bond + deposition) are added together to get the total deformation shown in the plot on the right. The slope of this graph is the "packaged strain" at -45 °C of Package Model C.

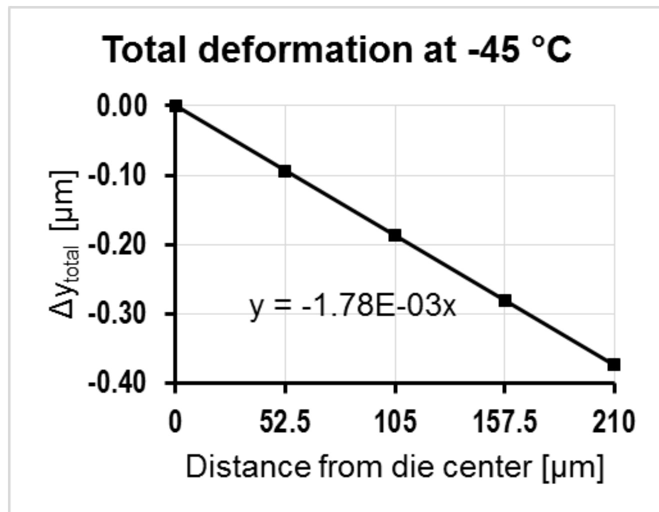

Figure 12: Sum of deformation values from all packaging steps and high temperature deposition as a function of distance form die center. The slope is the packaged strain at -45 °C.

Strain of packaged die across the operational temperature range

Sweeping the applied temperature—only on the plastic encapsulation step—and computing the sum of displacements along the scoped path resulting from all packaging steps, yields the strain across the operational temperature range (-45 °C to 155 °C) on all package models considered, plotted in Figure 13. Package models whose strain is the farthest from the unpackaged die are chosen (Packages A, B, and C), and linear best-fit equations are extracted for use in the subsequent modal analysis on the resonators. Additionally, as seen in Figures 14 (a) and (b), the packaged die deformation is isotropic, so the same displacement functions can be applied both in the lateral and transverse directions.

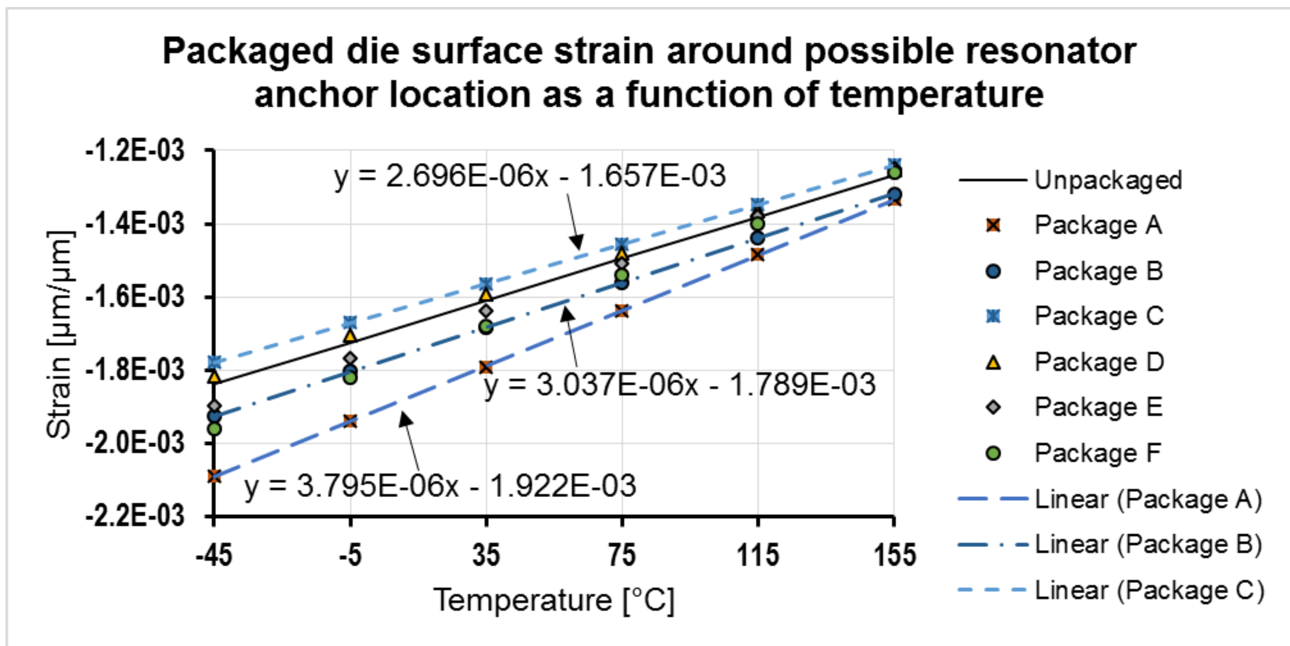

Figure 13: Lateral strain versus temperature for the unpackaged silicon die (solid black line) and packaged dies. Best-fit lines relate the strain to temperature, and these equations are used as nodal displacement functions for resonator anchors in the modal analysis

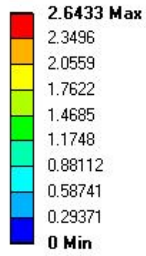

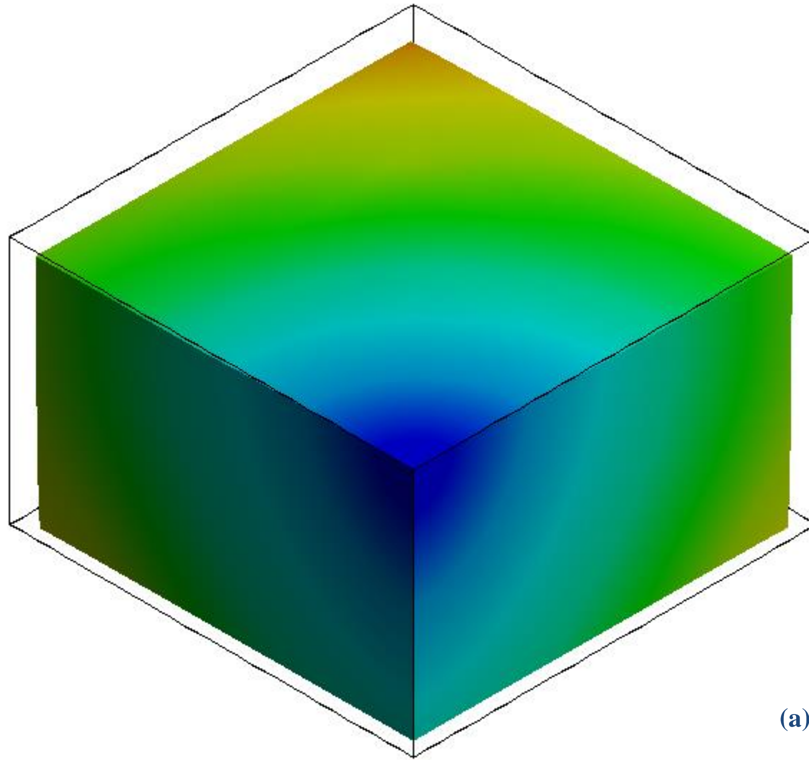

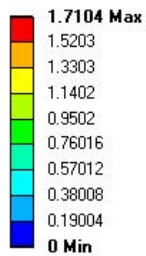

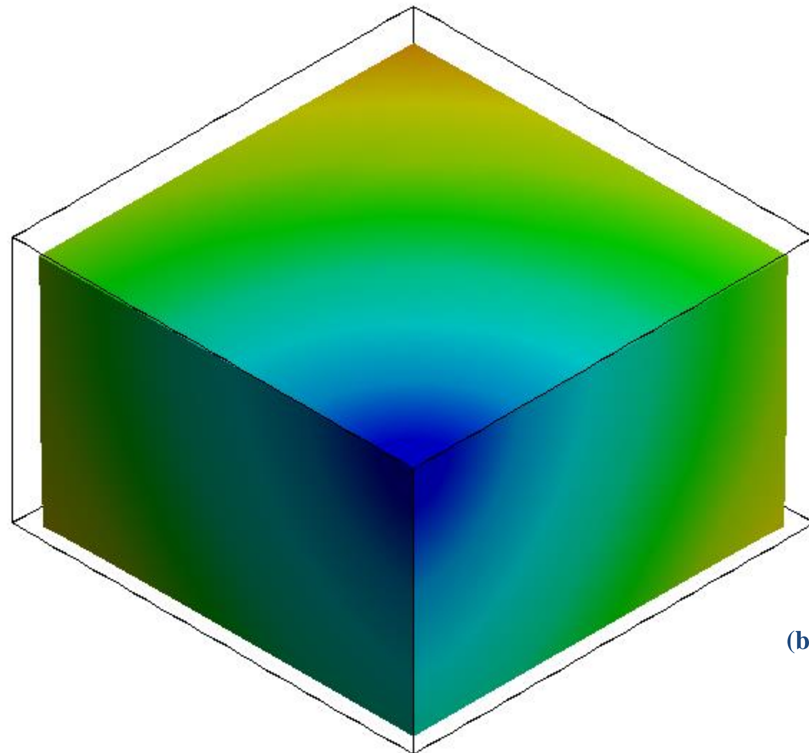

Figure 14: Total deformation of packaged wafer in package model C. (a) at -45 °C and (b) at 155 °C. Deformation is isotropic and warpage is insignificant.

Temperature dependence of resonant frequency

Variation of Young's modulus with temperature causes the resonant frequency of micromechanical resonators to be dependent on temperature. Additionally, since the resonator stiffness is susceptible to package-induced stress, thermal stability of both packaged and unpackaged micromechanical resonators must be simulated for comparison. The four geometries chosen for this work are 1) Clamped-clamped beam, 2) Free-free beam, 3) Center stem disk, and 4) Levitated disk.

ANSYS Mechanical [14] is used to simulate resonator temperature stability. Engineering data and geometry are defined in the Workbench interface as before. However, due to some limitations of the modal analysis in Workbench, this function is carried out through the use of APDL commands inserted in Mechanical. The code for the clamped-clamped beam is given as an example in Appendix C. Figures 15 and 17 show the quarter model of a clamped-clamped beam and a free-free beam resonator, respectively. As in the quarter package model, planes of symmetry are fixed in the direction normal to the plane and, since all package models showed minimal warpage on the packaged die surface, anchor nodes are fixed in the y-direction. Displacement as a function of the node x-coordinate and temperature for the unpackaged and packaged dies (taken from the trend lines of Figure 13) are expressed in Equations 1-4, where $U_{x,unp}$, $U_{x,A}$, $U_{x,B}$, and $U_{x,C}$ are the x-direction displacements of the unpackaged die, and packaged die in models A, B, and C, respectively, T is the stressed temperature (applied thermal condition), and x is the distance from die center.

$$U_{x,unp} = 2.85 \times 10^{-6}(T - 600) * x \tag{1}$$

$$U_{x,A} = (3.795 \times 10^{-6} \times T - 1.922 \times 10^{-3}) * x \tag{2}$$

$$U_{x,B} = (3.037 \times 10^{-6} \times T - 1.789 \times 10^{-3}) * x \tag{3}$$

$$U_{x,C} = (2.696 \times 10^{-6} \times T - 1.657 \times 10^{-3}) * x \tag{4}$$

The same equations are applied in the z-direction due to the isotropic nature of die deformation.

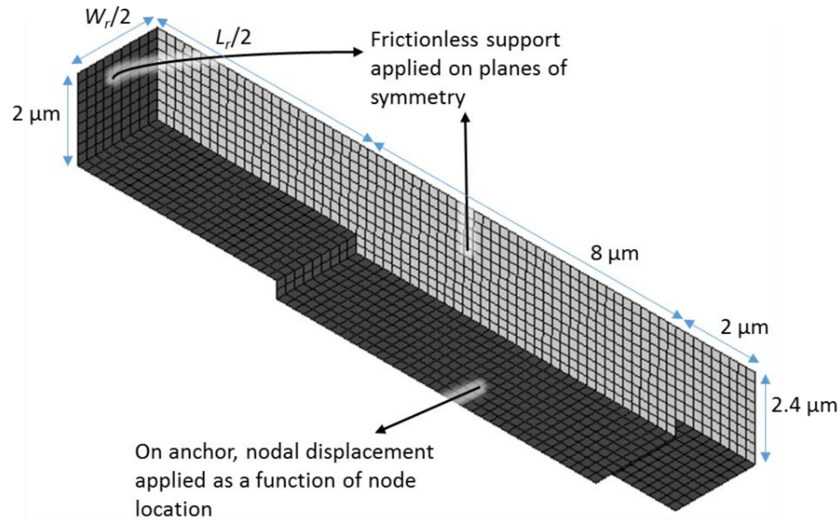

Figure 15: Finite element model showing solid elements of the clamped-clamped beam quarter model. Dimensions are given in Appendix A.

The finite element model is first solved for static loads (displacement and temperature), and the resulting deformation is examined to verify that the anchor moves by the amount predicted by Eqs. 1-4. By using the `PSTRESS` command, a stress stiffness matrix is calculated which is used in the subsequent prestressed modal analysis to determine the resonant frequency.

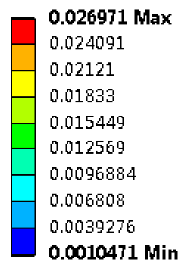

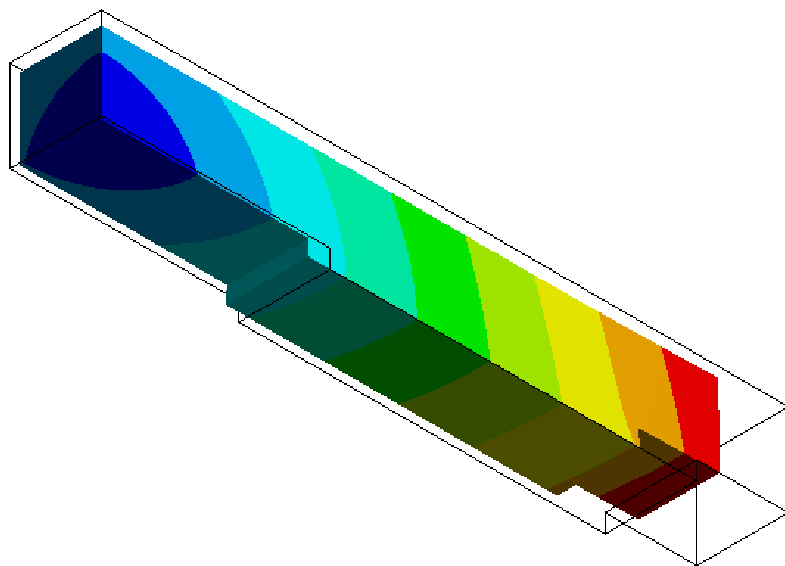

Figure 16: Static Deformation result showing CC beam anchor displacement due to package induced stress and applied temperature.

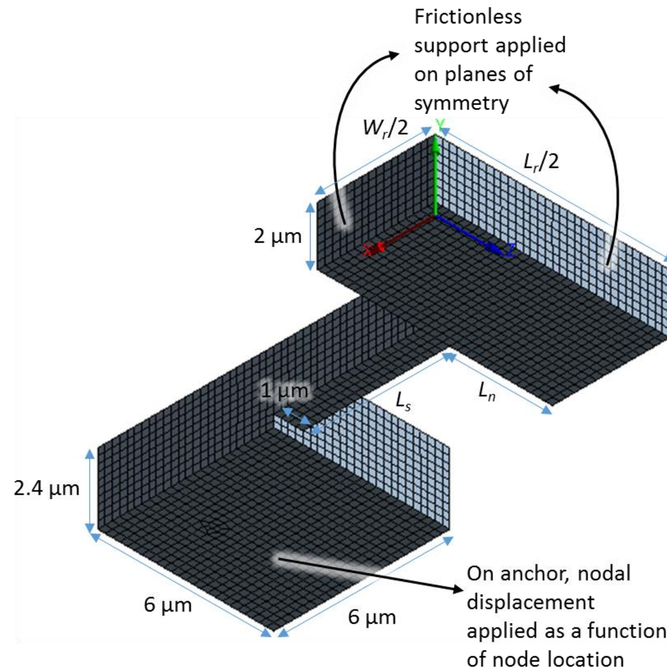

Figure 17: Finite element model showing solid elements of the free-free beam quarter model. Dimensions are given in the Appendix A.

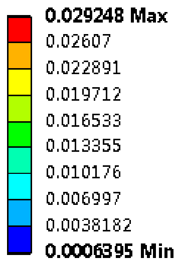

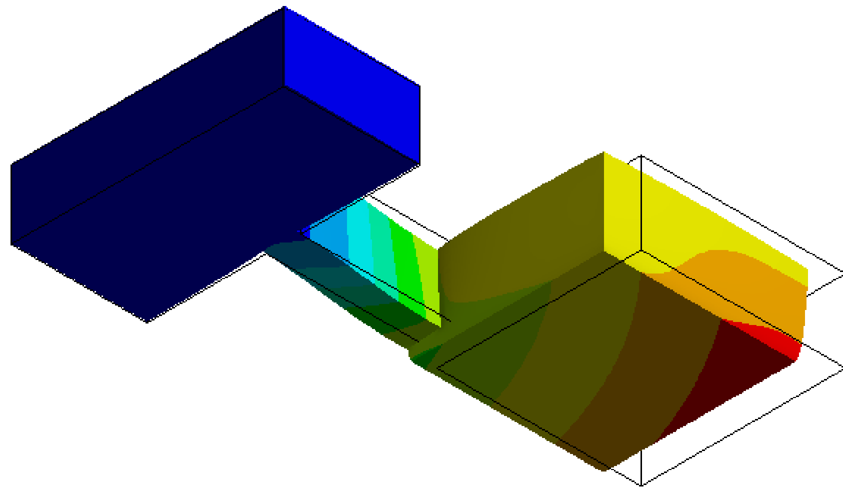

Figure 18: Static Deformation result showing an unpackaged FF beam anchor displacement due to cooling down from the stress free temperature of 600 °C to 22 °C.

After obtaining the static structural result and calculating stress stiffening effects, a modal analysis is now performed to calculate the resonant frequency of the desired mode shapes shown in Figure 19, determined using the Block Lanczos extraction method.

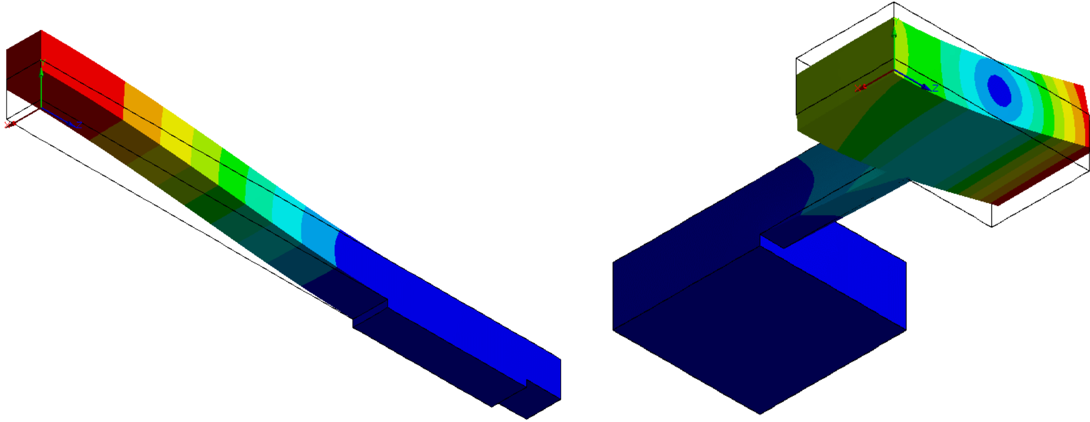

Figure 19: Desired mode shapes for the clamped-clamped and free-free beams

Unlike the beams, the disks selected for this work vibrate laterally. Mesh models and dimensions used for a centrally anchored disk and a disk levitated by four support beams on its perimeter, and their electrodes are shown in Figures 20 and 21. A static structural simulation shows that the lateral gap spacing changes significantly. The average gap spacing along the thickness of both disks is plotted in Figure 22.

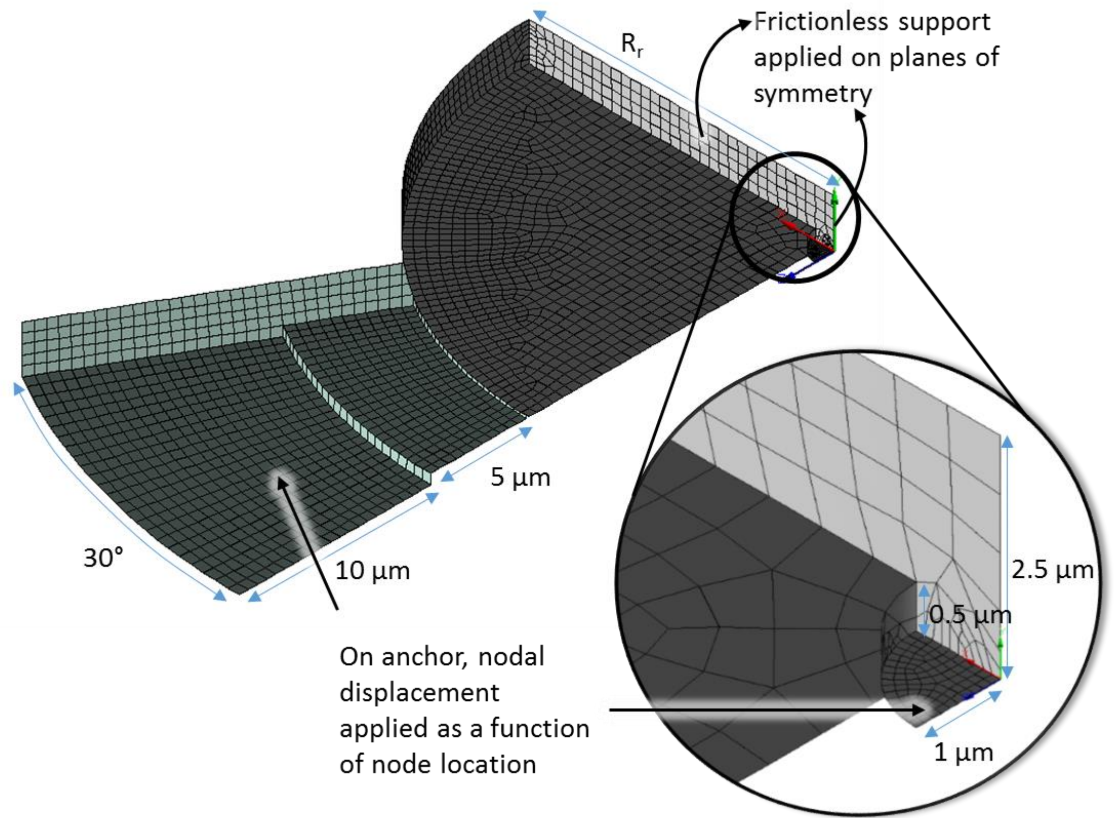

Figure 20: Finite element model showing solid elements of the centrally anchored disk quarter model. Dimensions are given in the Appendix A. The electrode is suppressed in the prestressed modal analysis.

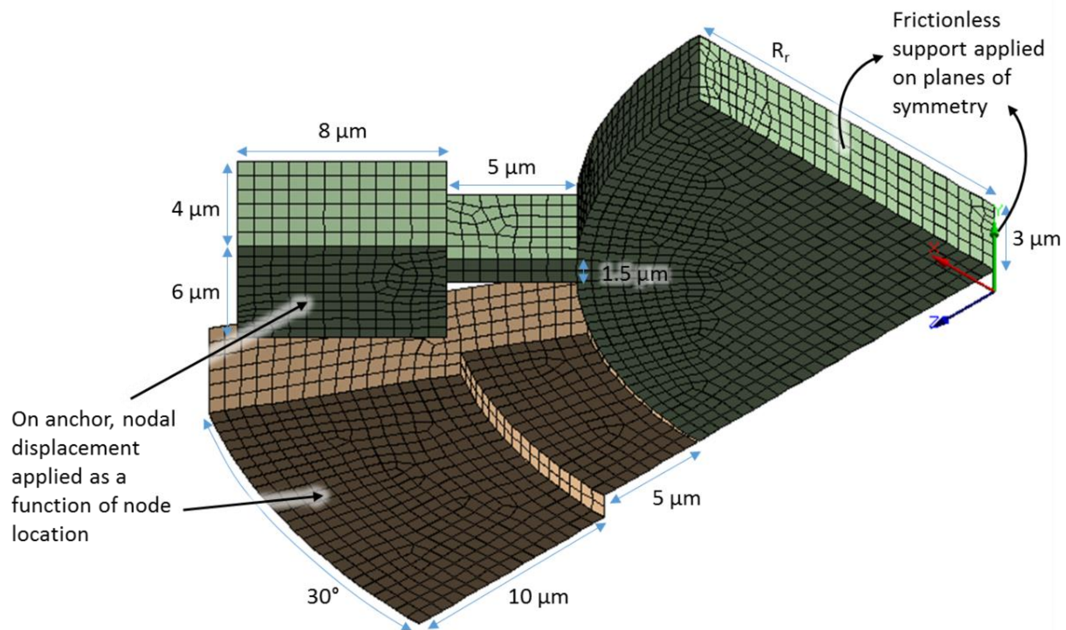

Figure 21: Finite element model showing solid elements of the levitated disk quarter model. Dimensions are given in Appendix A. The electrode is suppressed in the prestressed modal analysis.

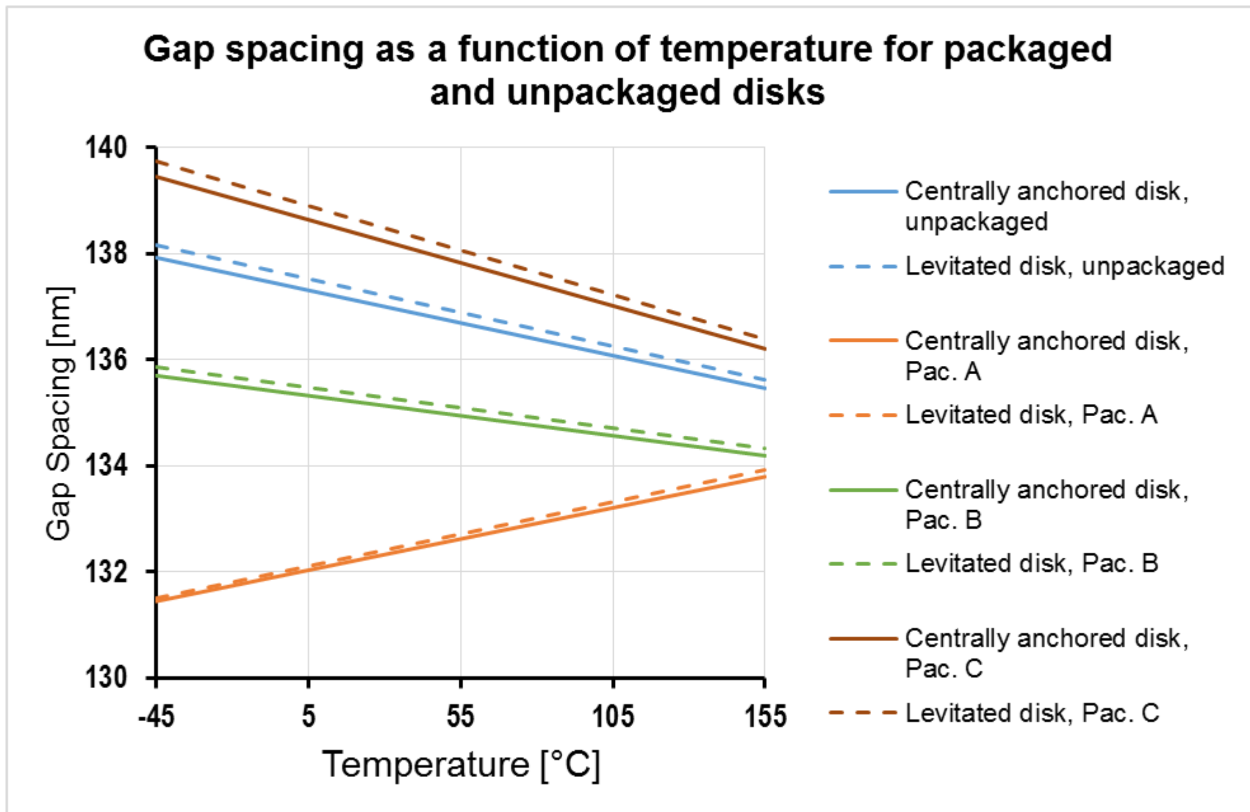

Figure 22: Gap spacing simulation results for the unpackaged and packaged disk resonators. The gap is 130 nm at the stress free temperature of 600 °C.

As with the beams, anchor displacement expressions and temperature loads are applied, and the natural frequency of disks is determined using the Block Lanczos extraction method. Mode shapes are shown in Figure 23.

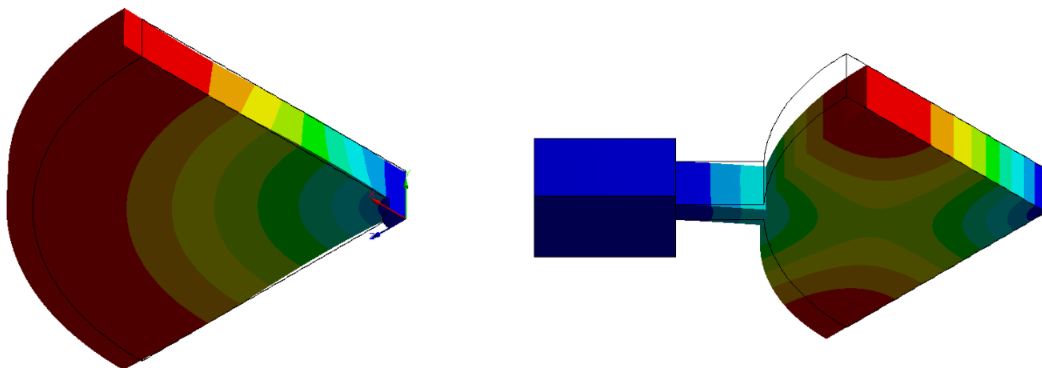

Figure 23: Desired mode shapes for the centrally anchored disk and levitated disk

Temperature Stability Results

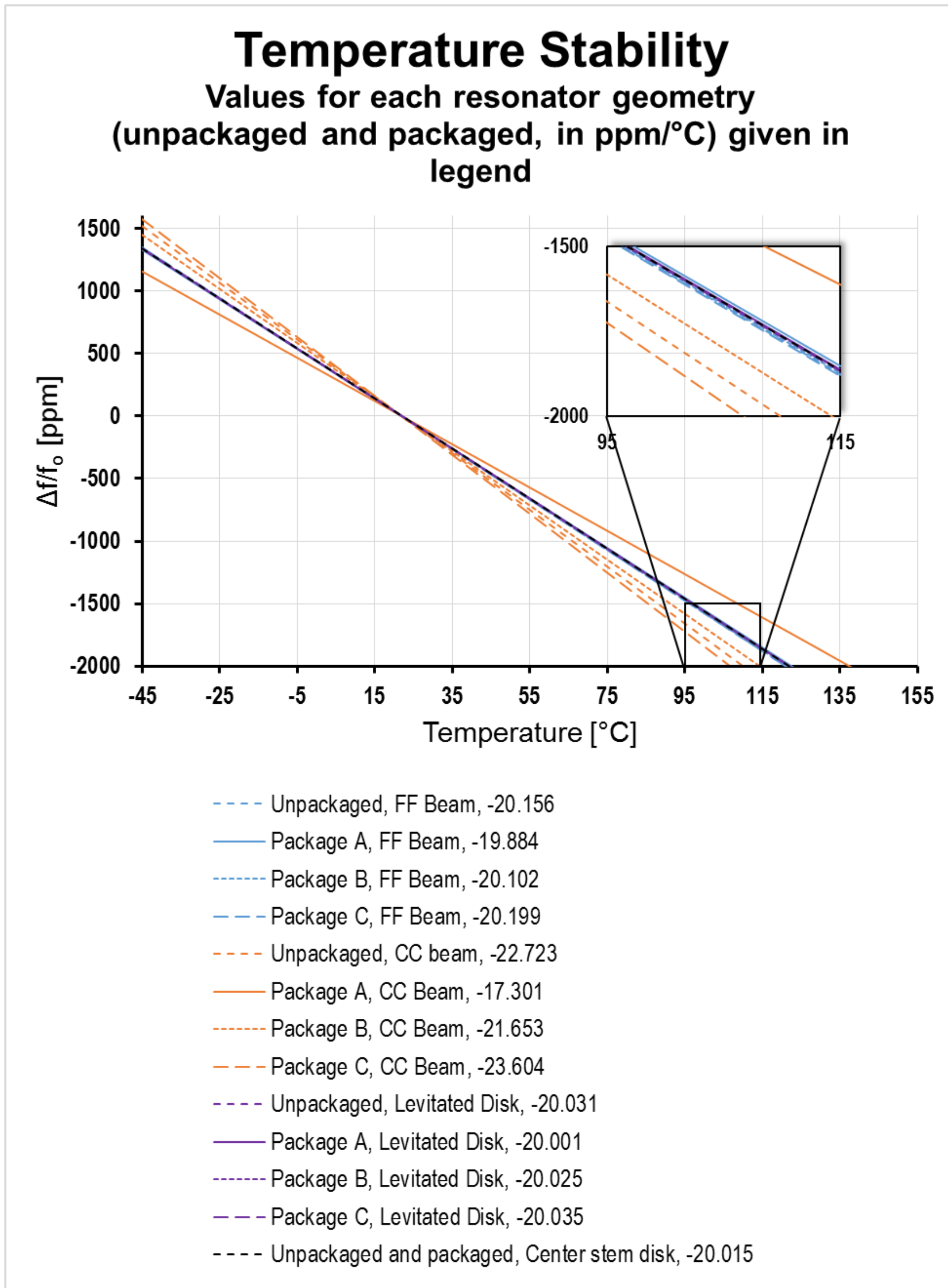

Figure 24: Temperature stability results for selected packaged and unpackaged resonators. Resonator dimensions are given in Appendix A.

Conclusion

The results in Figure 13 explain the effect of die attach and cap wafer material properties, and die and wafer cap thicknesses on package strain. Reducing t_{cap} and t_{die} to 300 μm and using Pyrex as the cap wafer material seems to improve micromechanical temperature stability, although it is detrimental to package strain. This is because, of the three die attach materials used, the die attach used in standard IC packaging, which has a relatively high thermal expansion coefficient, compared to silver glass and polyimide, introduces more stress in the die. No significant difference was found when the ceramic substrate thickness was reduced to 1 mm.

The slope of the package strain lines can be thought of as an "effective coefficient of thermal expansion, α_{eff}" which describes local behavior on the packaged die surface along the resonator anchor locations. Comparison of Figures 13 and 24 illustrates the direct correlation between α_{eff} and the temperature coefficient of frequency (TC_f), especially for the clamped-clamped beam. This is expected, because, of the various resonator geometries simulated, the CC beam is in direct contact with the substrate. Even though the FF beam has a large anchor area, it is levitated by support beams, and so, the package-induced stress related TC_f is very close to the unpackaged value. The mechanical frequency of disks is nearly impervious to package induced stress for the reason that their anchor area is small.

Gap spacing results of Figure 22 show that larger α_{eff} results in a smaller gap. Also, all gap spacing values measured are larger than the stress free gap of 130 nm. This is because the structural material thermal expansion coefficient of 3.35 ppm/°C is much larger than that of the silicon substrate, 2.85 ppm/°C, so the polysilicon shrinks faster than the silicon, increasing gap spacing. When α_{eff} is larger than the silicon CTE, like in Package A, gap spacing increases with temperature. From the earlier analysis of the resonant frequency of the pure mechanical system for the disks, the change in gap spacing due to package-induced stress would be the most significant cause of resonant frequency shift, rather than anchor shift.

Traditional package-induced stress simulations in microelectronics aim to estimate the effect of residual stress, on properties like the input offset voltage of a differential op amp, by

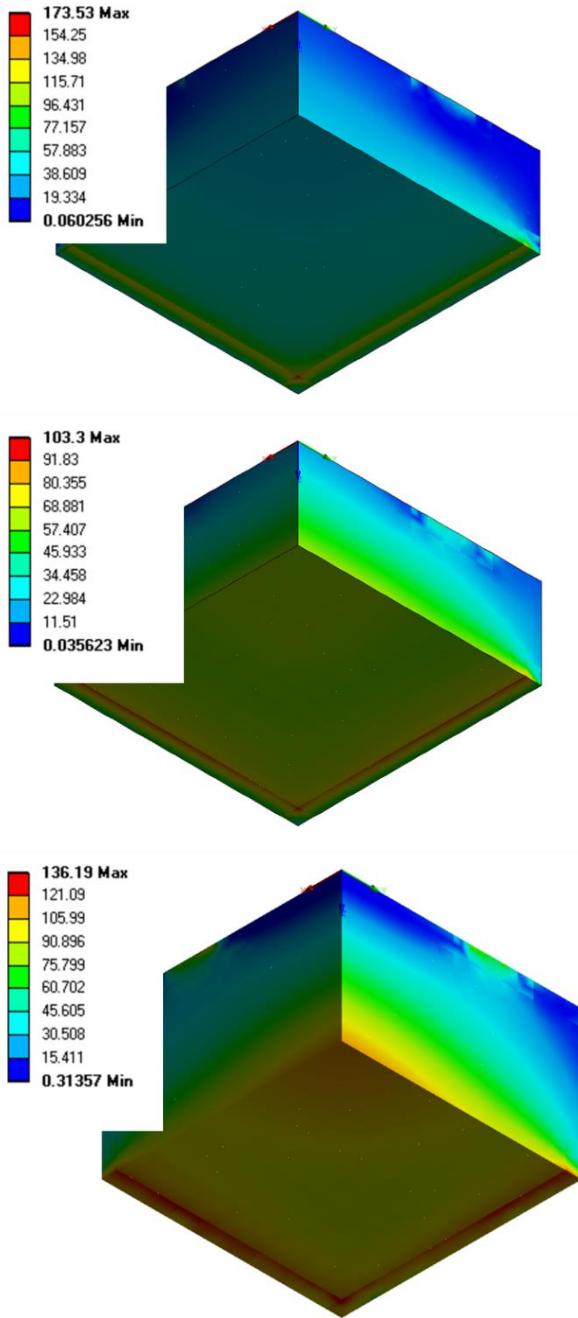

Figure 25: In-plane normal stress (in MPa) results of the dies in (a) Package A, (b) Package B, and (c) Package C

examining die deformation. Although the micromechanical resonator stiffness is only altered by the displacement of anchor nodes, residual stress still needs to be studied for possibilities of mechanical failure, in the form of delamination, when shear stress exceeds a certain limit, or crack formation. Figure 25, left, shows contour plots of in-plane stresses at 155 °C, σ, defined in (5) as the resultant of the x and y components of normal stress.

$$\sigma = \sqrt{\sigma_{xx}^2 + \sigma_{yy}^2} \tag{5}$$

The highest in-plane normal stress (175 MPa) appears in Package A, this value occurs at one corner of the die, and edge effects create a frame where the stress is around 115 MPa. The rest of the die sees very low stress values compared to the dies from the other packages. The die from Package C is under a very high stress value at its edge and the center contacting the die attach. This, together with the "effective α_{eff}" being less than the silicon substrate CTE, reveals that the silver glass restricts die deformation so much that the surface nodes displace less than they do in the unpackaged die.

Apart from failure testing, the major factors needed for a more sophisticated simulation include material property accuracy, thermal cycling, and a lack of perfect adhesion between materials. Often, material properties fall in a range of values, rather than being exact. This phenomenon can be an outcome of the manufacturing methods and can be measured experimentally, and must be accounted for in more accurate package

stress calculations. For example, varying levels of voltage across the glass wafer in an anodic bond leads to compositional gradients, yielding different coefficient of thermal expansion (CTE) values across the wafer [17]. Soft materials, such as die attach and polymer, have different CTE values above and below the glass transition temperature. Also, polymers, die attach materials, and glass undergo chemical shrinkage (also a time dependent property) in addition to thermal contraction. This is modeled by experimentally measuring the directional deformation as a function of stress free temperature and then using a CTE that varies with stress free temperature in the simulation [5].

Thermal cycling tests reveal time-dependent material properties, which can be used in a transient analysis. This is especially useful, since, in practice, after each processing step, the assembly is cooled down to room temperature before being heated back to the elevated temperature to prepare for the next packaging step. This would occur several times throughout the packaging process and during the lifetime of the package. The authors of [16] have determined that the residual stress in some materials is highly dependent on the "dwell time", the time that the assembly is subjected to a constant temperature. For soft materials such as the die attach adhesive and polymer, repeated heating and cooling may change the shape of the die attach and tilt the die (like in the X-ray images of [6]), resulting in an asymmetric package model.

Two possibilities can make the bonded contact assumption invalid. As discussed earlier, delamination may be a consequence of high shear stress, and can be simulated by slippage [5]. This model must be solved iteratively, by first calculating stress values resulting from a small temperature change, and then modifying contact elements that exceed the stress criterion, dictated by material properties, to non-bonded types in ANSYS (No separation, frictionless, frictional). This simulation must be repeated until the final temperature value. In the second case, the bonding material may have voids, resulting in loss of perfect adhesion [5] and can be modeled by a certain percentage of the contact area having a non-bonded contact type.

This work focusses on the temperature stability in sensors that are part of the original vision of a Smart Dust system [18], and hence, do not require further attachment to a printed circuit board (PCB). However, for applications such as cell phones and other portable electronics, where the packages are soldered to a PCB, additional stress is introduced due to the extra CTE mismatch. The PCB is also in tension since it's mounted on the outer frame of the target application. For such

cases, a good understanding of the target application and manufacturing process is required, in order to perform a more complete analysis on temperature stability of the packaged resonators.

While the simulation procedure presented in this report can be used as a rough estimate on how the choices of package materials and geometry affect resonator thermal stability, the package model can be made more accurate by using experimental data to gain more insight into material properties. In some cases, a transient analysis would also be required.

References

[1] V. Kempe, *Inertial MEMS: Principles and Practice*. New York: Cambridge University Press, 2011.

[2] R. Fraux, Reverse Costing Analysis Discera DSC 8002 MEMS Oscillator. System Plus Consulting, 2010.

[3] S. Nasiri and J. Seeger, “X-y axis dual-mass tuning fork gyroscope with vertically integrated electronics and wafer-scale hermetic packaging,” U.S. Patent 20050081633 A1, Oct 20, 2003.

[4] Small Precision Tools. Die Attachment Fluid Dispensing. [Online]. Available: http://www.smallprecisiontools.com/file/products/bonding/allcatalogues/Die%20Attachement%20and%20Fluid%20Dispensing%20-%20Catalogue%20-%20English.pdf

[5] G. Kelly, *The Simulation of Thermomechanically Induced Stress in Plastic Encapsulated IC Packages*. Boston: Kluwer Academic Publishers, 1999. Web.

[6] B.R. Simon, G. Sharma, S. A. Zotov, A. A. Trusov, and A. M. Shkel, “Intrinsic stress of eutectic Au/Sn die attachment and effect on mode-matched MEMS Gyroscopes,” *Inertial Sensors and Systems (ISISS), 2014 International Symposium on* , vol., no., pp.1,4, 25-26 Feb. 2014

[7] G. Li, A. A. Tseng, "Low stress packaging of a micromachined accelerometer," *Electronics Packaging Manufacturing, IEEE Transactions on* , vol.24, no.1, pp.18,25, Jan 2001

[8] S.S. Walwadkar and J. Cho, "Evaluation of Die Stress in MEMS Packaging: Experimental and Theoretical Approaches," Components and Packaging Technologies, IEEE Transactions on , vol.29, no.4, pp.735,742, Dec. 2006

[9] T. O. Rocheleau, T. Lin Naing, and C. T.-C. Nguyen, “Long-Term Stability of a Hermetically Packaged MEMS Disk Oscillator,” Proceedings, 2013 IEEE International Frequency Control Symposium, Prague, Czech Republic, Jul. 22-25, 2013

[10] SCHOTT North America, Inc., "High and Low Temperature Cofired Multilayer Ceramics (HTCC and LTCC)", Southbridge, MA, USA.

[11] DuPont™ GreenTape™ low temperature co-fired ceramic system, Figure 9.

[12] R. Kulke, M. Rittweger, and P. Uhlig. "LTCC – Multilayer Ceramic for Wireless and Sensor Applications"

[13] CoorsTek, Inc., The #05 Shank. [Online]. Available: http://www.nordson.com/de-de/divisions/dage/products/materialien/CoorsTek/Documents/CoorsTek_DieAttach.pdf

[14] ANSYS, Inc., *ANSYS 14.5*, Canonsburg, PA: 2012.

[15] E. Wang, T. Nelson, R. Rauch, "Back to Elements - Tetrahedra vs. Hexahedra," CAD-FEM GmbH, Munich, Germany.

[16] W. D. van Driel, G. Q. Zhang, J. H. J. Janssen, and L. J. Ernst, "Response Surface Modeling for Nonlinear Packaging Stresses," *Journal of Electronic Packaging*, vol. 125, no. 4, pp. 490, 497, Dec. 2003

[17] I. Sadaba, C.H.J. Fox, and S. McWilliam, "An Investigation of Residual Stress Effects due to the Anodic Bonding of Glass and Silicon in MEMS Fabrication," *Applied Mechanics and Materials*, vols. 5-6, Oct. 2006

[18] *Smart Dust: BAA97-43 Proposal Abstract*, POC: Kristofer S.J. Pister

Appendix A

Table 3: Beam frequency results and dimensions

	Frequency [MHz]							
	Free-free beam				Clamped-clamped beam			
	Unp	Pac. A	Pac. B	Pac. C	Unp	Pac. A	Pac. B	Pac. C
-45 °C	63.94978	63.94510	63.94817	63.95088	104.1048	103.9527	104.0526	104.1406
22 °C	63.86365	63.86015	63.86228	63.86456	103.9467	103.8326	103.9020	103.9763
155 °C	63.69235	63.69116	63.69144	63.69289	103.6325	103.5934	103.6027	103.6498
	Frequency Shift [ppm]							
-45 °C	1348.601	1330.296	1344.941	1351.49	1521.05	1156.763	1449.177	1580.17
22 °C	0	0	0	0	0	0	0	0
155 °C	-2682.33	-2646.13	-2675.09	-2688.04	-3023.32	-2303.03	-2881.13	-3140.31
	Thermal Stability [ppm/°C]							
	-20.1565	-19.8841	-20.102	-20.1995	-22.7232	-17.3014	-21.6531	-23.6037
	Dimensions [μm]							
L_r	16				10			
W_r	8				4			
t_r	2				2			
L_n	3.5							
L_s	5							
W_s	1							

Table 4: Disk frequency results and dimensions

	Frequency [MHz]							
	Center stem disk				Levitated disk			
	Unp	Pac. A	Pac. B	Pac. C	Unp	Pac. A	Pac. B	Pac. C
-45 °C	186.4931	186.4931	186.4931	186.4931	120.324	120.323	120.3236	120.3242
22 °C	186.2437	186.2437	186.2437	186.2437	120.1629	120.1622	120.1627	120.1631
155 °C	185.7476	185.7476	185.7476	185.7476	119.8426	119.8424	119.8424	119.8427
	Frequency Shift [ppm]							
-45 °C	1339.11	1339.094	1339.107	1339.112	1340.14	1338.164	1339.746	1340.451
22 °C	0	0	0	0	0	0	0	0
155 °C	-2663.56	-2663.53	-2663.55	-2663.57	-2665.6	-2661.69	-2664.82	-2666.21
	Thermal Stability [ppm/°C]							
	-20.0152	-20.015	-20.0152	-20.0153	-20.0306	-20.0012	-20.0247	-20.0352
	Dimensions [μm]							
R_r	16				16			
t_r	2				3			
L_s					5			
W_s					1.5			

Appendix B

To demonstrate the use of APDL command snippets in the package simulation, the following example is considered. At the die attach step, plastic solid elements and the plastic-to-ceramic contact pair are killed, and the reference temperature is now defined to be 350 °C, which overwrites the previously assigned stress free temperature.

The following APDL command is inserted under the plastic mold compound and die attach solid bodies to tag the solid plastic and die attach elements respectively.

```
*SET,EMC,MATID
*SET,DIE_ATTACH,MATID
```

The following APDL command is inserted under the plastic-to-ceramic contact pair to tag the contact and target elements accordingly.

```
MYCONT6=CID
MYTARG6=TID
```

Then, under the Static Structural environment, the `EKILL` command is used to kill the solid EMC elements and the EMC-to-LTCC contact and target elements. Note that killing a solid element multiplies its stiffness by 10^{-6} and does not actually delete the element from the model. `MP, REFT` overwrites the previously assigned stress free temperature

```
ALLSEL, ALL
ESEL, S, MAT,,EMC
ESEL, A, TYPE,, MYCONT6
ESEL, A, TYPE,, MYTARG6
EKILL, ALL
MP, REFT, DIE_ATTACH, 350,
```

Appendix C

```
!! ANSYS APDL COMMANDS FOR PRESTRESSED MODAL ANALYSIS OF A CLAMPED-CLAMPED
!! BEAM THIS BEAM MODEL INCLUDES TRANS126 ELEMENTS TO INCORPORATE
!! ELECTRICAL STIFFNESS

ANTYPE, STATIC                                  ! SET ANALYSIS TYPE TO
                                                ! STATIC

ALLSEL, ALL                                     ! SELECT EVERYTHING
NSEL, S, LOC, Y, 0                              ! SELECT ANCHOR NODES
CM, ANCHOR, NODE                                ! GROUP SELECTED NODES INTO
                                                ! A COMPONENT NAMED "ANCHOR"

CMSEL, S, ANCHOR, NODE                          ! SELECT NODES OF COMPONENT
                                                ! "ANCHOR"
*GET, NCOUNT, NODE, 0, COUNT                    ! OBTAIN NUMBER OF NODES IN
                                                ! COMPONENT "ANCHOR"
*GET, NCURRENT, NODE, 0, NUM, MIN               ! COUNTER TO SAVE THE
                                                ! SELECTED NODE NUMBER
*DO, I, 1, NCOUNT                               ! LOOP THROUGH NODES


! APPLY X-DISPLACEMENT, DETERMINED BY THE PACKAGE MODEL
! THAT VARIES WITH X-COORD AND TEMPERATURE ARG2
D, NCURRENT, UX, (ARG3*ARG2-ARG4)* NX(NCURRENT)

! APPLY Z-DISPLACEMENT, DETERMINED BY THE PACKAGE MODEL
! THAT VARIES WITH Z-COORD AND TEMPERATURE ARG2
D, NCURRENT, UZ, (ARG3*ARG2-ARG4)* NZ(NCURRENT)


CMSEL, S, ANCHOR, NODE                          ! SELECT NODES OF COMPONENT
                                                ! "ANCHOR"

NCURRENT=NDNEXT(NCURRENT)                       ! SELECT NODE HAVING A NODE
                                                ! NUMBER GREATER THAN
                                                ! NCURRENT

*ENDDO                                          ! END DO-LOOP

ALLSEL, ALL                                     ! SELECT EVERYTHING
CMSEL, S, ANCHOR, NODE                          ! SELECT NODES OF COMPONENT
                                                ! "ANCHOR"
D, ALL, UY, 0                                   ! FIX Y-DISP OF ANCHOR

ALLSEL, ALL                                     ! SELECT EVERYTHING
CMSEL, U, ANCHOR, NODE                          ! UNSELECT "ANCHOR"

BF, ALL, TEMP, ARG2                             ! APPLY TEMPERATURE OF VALUE
```

```
                                        ! ARG2 TO SELECTED NODES

ALLSEL, ALL                             ! SELECT EVERYTHING
PSTRESS,ON                              ! CALCULATE PRESTRESS
                                        ! EFFECTS

SOLVE                                   ! OBTAIN STATIC SOLUTION
FINISH                                  ! EXIT SOLUTION PROCESSOR
                                        ! AND SAVE RESULTS

/SOLU                                   ! ENTER SOLUTION PROCESSOR

ANTYPE,MODAL                            ! SET ANALYSIS TYPE TO MODAL
PSTRESS, ON                             ! INCLUDE PRESTRESS EFFECTS
ALLSEL,ALL                              ! SELECT EVERYTHING
MODOPT, LANB, 6, 0, 100E6               ! SPECIFY ANALYSIS OPTIONS
MXPAND                                  ! WRITE ALL MODES WITHIN
                                        ! FREQUENCY RANGE SPECIFIED
```

In the above code, ARG3, ARG2, and ARG4 are parameters that refer to package model (taken from the trend lines of Figure 13) and temperature variables, as in the following table:

Table 5: Design points that control anchor displacements in the modal analysis

Applied Temperature, ARG2 [°C]	ARG3	ARG4
Unpackaged		
-45	2.850E-06	1.710E-03
22	2.850E-06	1.710E-03
155	2.850E-06	1.710E-03
Package A		
-45	3.795E-06	1.922E-03
22	3.795E-06	1.922E-03
155	3.795E-06	1.922E-03
Package B		
-45	3.037E-06	1.789E-03
22	3.037E-06	1.789E-03
155	3.037E-06	1.789E-03
Package C		
-45	2.696E-06	1.657E-03
22	2.696E-06	1.657E-03
155	2.696E-06	1.657E-03